International Journal of Nanomedicine

Dovepress

open access to scientific and medical research

Open Access Full Text Article

ORIGINAL RESEARCH

Assessing the axonal translocation of CeO_2 and SiO_2 nanoparticles in the sciatic nerve fibers of the frog: an ex vivo electrophysiological study

This article was published in the following Dove Press journal:
International Journal of Nanomedicine
19 November 2015
Number of times this article has been viewed

Georgia Kastrinaki[1,*]
Christos Samsouris[2,*]
Efstratios K Kosmidis[3]
Eleni Papaioannou[1]
Athanasios G Konstandopoulos[1,4]
George Theophilidis[2]

[1]Aerosol and Particle Technology Laboratory (APTL), CERTH/CPERI, Thessaloniki, Greece; [2]Laboratory of Animal Physiology, School of Biology, Aristotle University of Thessaloniki, Thessaloniki, Greece; [3]Laboratory of Physiology, Department of Medicine, Aristotle University of Thessaloniki, Thessaloniki, Greece; [4]Department of Chemical Engineering, Aristotle University of Thessaloniki, Thessaloniki, Greece

*These authors contributed equally to this work

Abstract: The axonal translocation of two commonly used nanoparticles in medicine, namely CeO_2 and SiO_2, is investigated. The study was conducted on frog sciatic nerve fibers in an ex vivo preparation. Nanoparticles were applied at the proximal end of the excised nerve. A nerve stimulation protocol was followed for over 35 hours. Nerve vitality curve comparison between control and exposed nerves showed that CeO_2 has no neurotoxic effect at the concentrations tested. After exposure, specimens were fixed and then screen scanned every 1 mm along their length for nanoparticle presence by means of Fourier transform infrared microscopy. We demonstrated that both nanoparticles translocate within the nerve by formation of narrow bands in the Fourier transform infrared spectrum. For the CeO_2, we also demonstrated that the translocation depends on both axonal integrity and electrical activity. The speed of translocation for the two species was estimated in the range of 0.45–0.58 mm/h, close to slow axonal transportation rate. Transmission electron microscopy provided direct evidence for the presence of SiO_2 in the treated nerves.

Keywords: CeO_2, SiO_2, FTIR, nanoparticles, ex vivo electrophysiology, frog sciatic nerve, translocation

Introduction

Nanoscience, the study of nanoscale materials and their applications, is a modern, multidisciplinary approach with promising results across several scientific fields including the catalytic and energy sector[1–4] and is gradually established in many commercial products. In medicine, drug delivery with nanoparticles (NPs) is one of most dynamically evolving research areas.[5] However, fundamental understanding of issues related to toxicity and environmental impact of nanoscale materials is still under investigation.[6] During the past several years, there have been numerous toxicological investigations of airborne NPs and their impact on occupational health and the environment.[7–9] Experimental models have provided clear evidence that NPs can not only translocate to organs after inhalation,[10–12] but can also cause disruption of the blood–brain barrier through different administration routes, including the intravenous, the intraperitoneal, and the intracerebral route.[13,14] Inhaled NPs either translocate directly into the brain or exit the lungs and enter the circulation as shown in rat experiments.[8]

The nerve fibers of the olfactory nerve is the route of entry of NPs to the brain.[14] Silver,[15] ultrafine carbon black,[16] manganese oxide,[10] and titanium dioxide (TiO_2)[17,18] NPs have all been found to translocate into the brain via the olfactory nerve in rodents. These NPs are reported to cause inflammation and impair neural function in the hippocampus. It has been suggested that, despite differences between rodent and

Correspondence: Efstratios K Kosmidis
Department of Medicine, Aristotle University of Thessaloniki, Thessaloniki 54 124, Greece
Tel +30 231 099 9240
Fax +30 231 099 9239
Email kosmidef@med.auth.gr

human olfactory systems, this pathway may be relevant in humans.[10] It has also been suggested that nanogold particles cross into the cerebrospinal fluid space after axonal transport to the olfactory bulb and are distributed to different brain areas.[19] Deregulation of axonal transport mechanisms is involved in a number of neurodegenerative diseases. It is therefore imperative to further investigate the effects and mechanisms of NP transportation in nerve fibers. Studying NP's mobility in nerve fibers is essential for reasons beyond neurotoxicity, since NPs can be used as possible drug carriers. Furthermore, they can provide information about the quality of axonal transport and are also a significant parameter to assess proper function of nerve fibers.

Silicon-based particles have been long approved for medical use,[20] by employing SiO_2 matrices as delivery systems[21–27] for protein, enzymes, drugs, and genes. CeO_2 (ceria) NPs on the other hand were recently studied for their pharmacological potential[28] as drug delivery carriers by exploiting their multienzyme antioxidant mimetic properties.[29] Divergent studies though have shown both beneficial and toxic effects,[30–33] requiring additional studies for biocompatible standardization.

The purpose of this work was to use an ex vivo nerve preparation based on the isolated frog sciatic nerve in order to study in detail the movement of CeO_2 and SiO_2 NPs in the nerve fibers of the peripheral nervous system.

Material and methods

The sciatic nerve preparation

Frogs (*Rana ridibunda*) of either sex and of the same age (ranging from 12 to 15 months), weighing 40–60 g, were used. The frogs were euthanatized (decapitated and pithed), and the sciatic nerves were dissected from the spinal cord to the knee, immersed in standard physiological saline solution, and cleaned under a dissection microscope. All experimental procedures were conducted in accordance with the protocols outlined by the Aristotle University of Thessaloniki, Greece, regarding the recommended standard practices for Biological Investigations. When required, the epineural sheath was removed. The composition of the saline was (in mmol/L): NaCl 135, KCl 4.7, $CaCl_2$ 2.4, $MgCl_2$ 1.1, $NaHCO_3$ 1.0, HEPES 10, glucose 11 (pH 7.4). The nerve was mounted across a three-chambered recording bath, made of Plexiglas, a diagram of which is shown in Figure 1A. The recording bath has been used in a variety of ex vivo neurotoxicological studies and it is fully described elsewhere,[34–36] but a short description will be given below in order to clarify the protocol for the exposure of the nerve to NPs. The recording bath consists of three chambers: 1) the stimulating chamber (S in Figure 1A) where the proximal cut end of the nerve (Figure 1B) and the active stimulating electrode were placed. The stimulating electrode was connected to a constant voltage stimulator (Digitimer, DS9A; Digitimer Ltd, Welwyn Garden City, UK); 2) the perfusion chamber (n in Figure 1A), where the middle of the nerve was immersed and the grounds of the recording and stimulating electrodes were placed; and 3) the recording chamber (R in Figure 1A), where the distal end of the nerve and the active electrode of an AC (alternating current) differentiate amplifier (Neurolog, NL822; Digitimer Ltd) were placed. Gold electrodes of 24 carat were used. The dimensions of each chamber were 22×22×10 mm (length, width, depth), allowing a solution volume of 10 mL. The three chambers were next to each other, separated by two partitions of 2 mm width (part in Figure 1A).

Sciatic nerve electrophysiology

For the electrophysiological experiments and the application of NPs, a waterproof insulation between the three parts of the nerve (proximal, middle, and distal) was required. This was necessary to obtain a constant amplitude in nerve compound action potential (CAP) for a long period of time and to eliminate the possibility of any transport of NPs from one chamber to another.[37] For this purpose, the top of each partition, including a part of the nerve at the top, approximately 2 mm long, was smeared with a layer of 1–2 mm thick impression paste Xantopren, Heraeus Kulzer, Germany (Xanth in Figure 1A), while a glass cover (c in Figure 1A) was placed on top of the nerve and the impression paste. Thus, the part of the nerve on the partition and the impression paste were sandwiched between the glass cover (c) and the top of the partition. The impression paste Xantopren, used extensively in dentistry, was found to have the smallest impact on the vitality of the nerve compared to other similar materials.[35] When the impression paste solidified, the three chambers were filled once to cover the part of the nerve in each chamber with oxygenated saline (O_2 100%). The saline was stagnant in the three chambers for the rest of the experiment. The temperature of the saline was constantly maintained at 24°C±1°C using a cooling–heating system of water running below the perfusion chamber. To record nerve activity, we generated CAP (Figure 1C) using continuous electrical stimulation of 1 Hz. The constant-voltage stimuli were supramaximal (duration: 0.05 milliseconds and amplitude: 2–3 V), 2–3 times higher than the stimulus intensity required to generate the maximum CAP. Throughout the text, the term CAP refers to maximum CAP recorded using the AC amplifier.

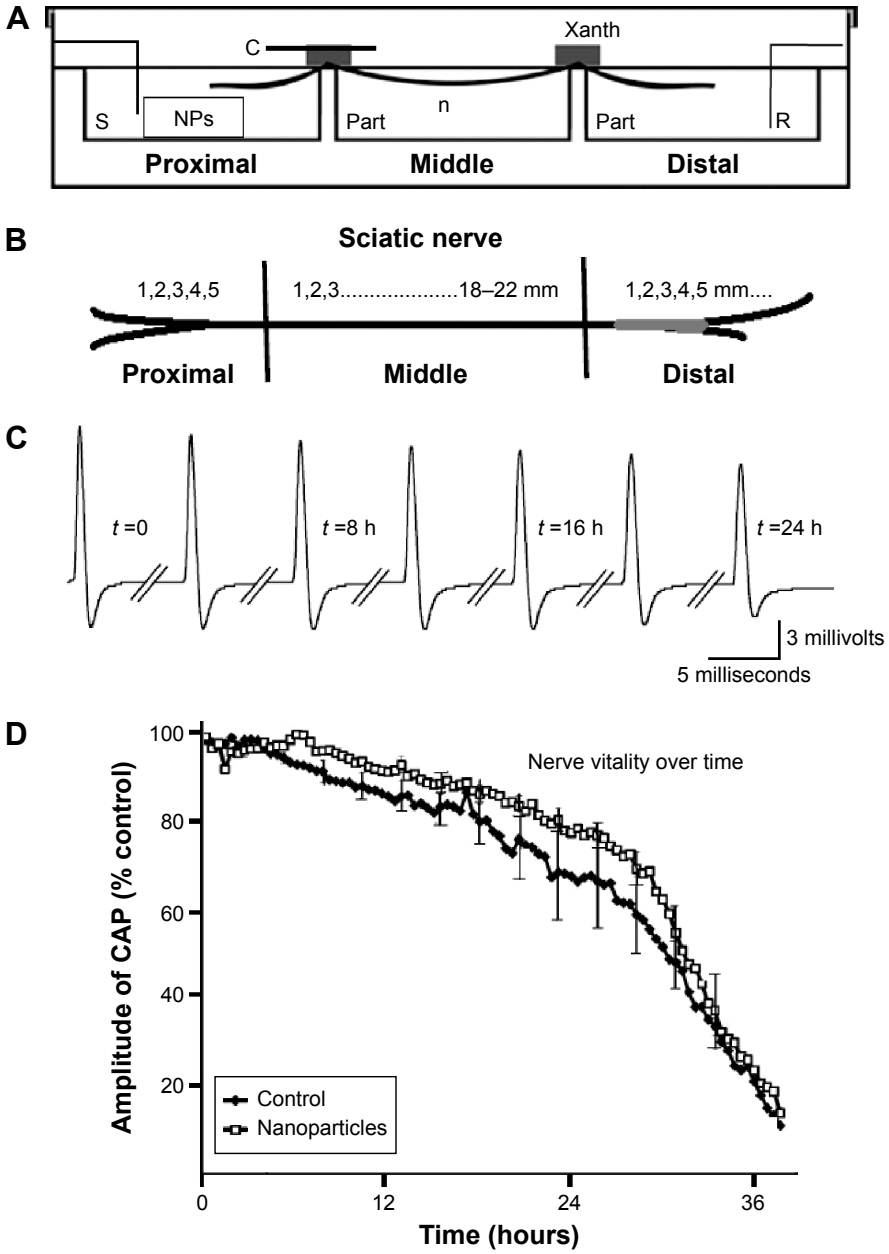

Figure 1 Experimental setup and electrophysiology.
Notes: (**A**) Recording bath scheme. (**B**) Schematic representation of sciatic nerve's proximal, middle, and distal regions. (**C**) Indicative evoked CAPs from whole nerve recordings. (**D**) Nerve vitality curve for CeO_2.
Abbreviations: C, glass cover; CAP, compound action potential; n, perfusion chamber; NPs, nanoparticles; part, partition; R, recording chamber; S, stimulating chamber; Xanth, Xantopren; h, hours.

The output of the amplifier was fed to a computer through a data acquisition card interface (Keithley KPCI 3102; Keithley Instruments, Cleveland, OH, USA). The software was designed using Labview (Labview 5.1, National Instruments, Austin, TX, USA).

Synthesis, application, and observation of CeO_2 and SiO_2 NPs

NPs were synthesized by an aerosol spray pyrolysis unit used for the synthesis of tailor-made NPs.[38] In aerosol spray pyrolysis, a precursor solution is atomized into fine droplets, which undergo evaporation of solvent and gradual precipitation of the precursor as they pass through a tubular heated reactor. A quartz fiber filter at the exit of the reactor collects the synthesized particles. The precursor solution for the CeO_2 particles was an aqueous 6 M solution of $CeCl_3 \cdot 7H_2O$ (ACROS Organics, New Jersey, NJ, USA). The synthesis temperature of the tubular reactor was 500°C, and the gas flow rate was 7 L/min, while the collected particles were calcined at 700°C for 2 hours. The particles were

characterized by transmission electron microscopy (TEM, JEOL JEM 2010; JEOL USA, Inc, Peabody, MA, USA) for their morphology, which was spherical and dense with a diameter size distribution from 110 to 250 nm. Their structure was polycrystalline.

SiO_2 particles were synthesized from a precursor solution of TEOS (Fluka)/EtOH/H_2O in molar ratios of 1/9.9/63.3. The synthesis temperature was 500°C in 7 L/min flow rate, while the particles were calcined at 550°C/4 hours. The SiO_2 NPs were characterized by TEM (JEOL JEM 2010) for their morphology. The TEM image also depicts spherical dense particle morphology with diameter size distribution between 30 and 120 nm, while their crystallinity is amorphous.

In order to study the transport of CeO_2 and SiO_2 NPs in the axons of the peripheral nerve, the NPs were diluted in saline and placed in the stimulating chamber, where the proximal end of the nerve was immersed. Before application, the edge of the proximal part was cut again using sharp fine microscissors, and the cut end was exposed to double distilled water for 3 minutes in order to open the cut ends of the nerve fibers. The CeO_2 or SiO_2 NPs were supplied at the final concentration of an aqueous distilled water pH =7 solution of 1.7 g/L concentration and were diluted eight times when applied in the stimulating chamber, where the proximal cut end of the nerve was placed (final concentration: 0.21 g/L). The particles were not charged by surface treatment in order to avoid particle movement by stimulation voltage. Under these conditions, the nerve was continuously stimulated. When the amplitude of CAP reached values below 20% of its original amplitude, usually after 36 hours, the experiment was terminated, the nerve was washed with distilled water and fixed using 20% glutaraldehyde for 12 hours.

For the observation with Fourier transform infrared (FTIR) microscopy, the fixed nerves were cut in three parts, the proximal, middle, and distal (Figure 1B), and dried in 100°C for 2 hours before observation in an FTIR microscope (Smiths-IlluminatIR, Smiths Detection, Hertfordshire, UK) at 600–4,000 cm^{-1} wavenumber. An automated, computer-handled holder can adjust the location of the different sample regions, thus, the whole nerve length was scanned by taking a spectrum every 1 mm and identifying the regions with NP presence. Every absorption spectrum range covers approximately 100 μm diameter region. For the observation with TEM, the part of the nerve (with mm precision) that exhibited NPs presence by FTIR characterization was cut and dried for 2 days in 100°C. The dried piece was pestled and the nonmembrane material was collected and diluted in ethanol for dropping it on the TEM carbon holder. The holder was left to dry under ambient conditions before loading it in the vacuum chamber.

Data analysis – statistics

As an indication of the proper physiological function of the nerve fibers of the isolated sciatic nerve, samples of the evoked CAP were digitized and stored in a computer every 30 minutes throughout the experiment, usually lasting over 36 hours. The amplitude of the CAP was measured from baseline to peak and expressed as a percentage of the amplitude of the CAP after 1 hour equilibration of the nerve. The percentage values were expressed as mean and standard error mean. The outcomes of many trials using different nerves were averaged and plotted against time as the vitality curve, or the time–response curve. For the eight experiments in which the nerves were exposed to CeO_2, the values of the CAP, measured every 30 minutes, were expressed as means and standard error mean and were used to plot the time–response curve. When required, data were analyzed by one-way analysis of variance (ANOVA) and Bonferroni's post hoc tests. We determined significance using Student's *t*-test or ANOVA, as appropriate ($P<0.05$).

Chemicals

We purchased KCl, NaCl, and $MgCl_2$ from Panreac (Barcelona, Spain), HEPES from BiochemicaFluka (Fluka, Switzerland), glucose from Riedel-de Haen (Seelze, Germany) and $NaHCO_3$ from Merck (Darmstadt, Germany), and $CeCl_3 \cdot 7H_2O$ from ACROS Organics.

Results

The nerve preparation

In normal solution, CAP amplitude remained constant for nearly 12 hours and then gradually declined (Figure 1C). The gradual decrease in amplitude is due to an accumulating number of axons losing the ability to conduct action potentials over time. On average, CAPs reached 20% of their initial amplitude in 36 hours (n=6) as shown in the vitality curve, in Figure 1D (filled squares). For NP mobility evaluation, the stimulating bath with the proximal nerve was filled with physiological solution with CeO_2 NPs at a concentration of 0.21 g/L. To exclude the possibility of any toxic effects of CeO_2 NPs on the exposed part of the nerves, the vitality curve for the particular case was plotted (Figure 1D, open squares). This curve (n=8) displayed similar characteristics with the control, and no statistically significant difference was seen ($P>0.05$), although a small protective trend can be observed for CeO_2. This is an indication that at the relatively

small concentrations used in our study (0.21 g/L), there is no toxic effect on the proximal part of the nerve.

CeO_2 NPs translocate in the sciatic nerve fibers

In this study, eight nerves were exposed to CeO_2 NPs and screen scanned using the FTIR microscope, as described. The FTIR absorption spectrums of a nonexposed nerve and of the pure CeO_2 NPs were used as negative and positive controls, respectively. No traces of CeO_2 NPs were detected in the untreated nerves.

In six out of eight treated nerves, CeO_2 NPs translocated within the nerves. CeO_2 was observed mainly in the middle and distal regions of the nerve. In all six nerves, no NPs were observed in the proximal region. In the other two nerves, there was no transport. In Figure 2, exemplary FTIR traces are shown from such an experiment. The bottom trace is the negative control (control nerve, free of NPs) and the trace at the top (CeO_2 NPs) the positive. CeO_2 NPs presence is indicated with arrows. The nerve was screened scanned every 1 mm. The middle FTIR trace (Figure 2, no CeO_2) is indicative of the proximal, distal, and of the first 13 mm of the middle part, where no NPs were detected, (compare traces marked with no CeO_2 and CeO_2). It is worth mentioning that the absorption spectrum indicating the presence of CeO_2 NPs appeared only in a short region as a bundle at the middle part of the nerve (insert at the right of Figure 2). In this particular case, NPs were located between 14 and 15 mm of the middle part (according to Figure 1B). The difference in size of the CeO_2 characteristic peak at 600–800 cm^{-1} indicates that at 14 mm (low CeO_2 trace), the concentration of CeO_2 NPs is lower than at 15 mm (high CeO_2 trace). Although the exact terminal positioning of the NPs differed among the six nerves examined between 14 and 20 mm, a constant observation was that CeO_2 NPs tended to cluster and travel together as a bundle.

Another less typical set of recordings is demonstrated in Figure 3, where it seems that NPs reached the beginning of the distal region (1–2 m, according to Figure 1B), far from their usual position at the 15–20 mm region of the middle part, while a bundle of NPs is also located at the far distal part (at 4–5 mm).

All the aforementioned experiments were terminated when the CAP reached a value of 20% of its initial value in 36–40 hours, and the nerves were fixed eliminating any further translocation. Thus, the appearance of NPs at the far end of the middle part allowed us an approximate estimation of the speed of their movement inside the nerve fibers. Our results indicate an average NPs translocation speed of 0.45–0.58 mm/h.

CeO_2 NPs translocate through the nerve fibers exclusively

In order to verify that NPs were translocated only through the axons and not along the other elements of the sciatic nerve, such as the epineurium (perineural sheath), perineurium, and endoneurium, the nerve fibers were damaged by applying a slight pressure on the nerve using the tip of a fine forceps. The pressure was enough to damage the nerve fibers since the transmission of the electrically generated CAP along the sciatic nerve was completely eliminated; a CAP was never recorded from the four nerves tested even after 40 hours of continuous recordings. Care was taken so the lesion was enough to damage the nerve fibers, but not enough to cause any damage on the structures surrounding and protecting the nerve fibers. No CeO_2 NPs translocation was observed in all four damaged nerves tested.

To ensure that NPs enter the nerve fibers only from their cut end, the middle part of the nerve incubated in the middle

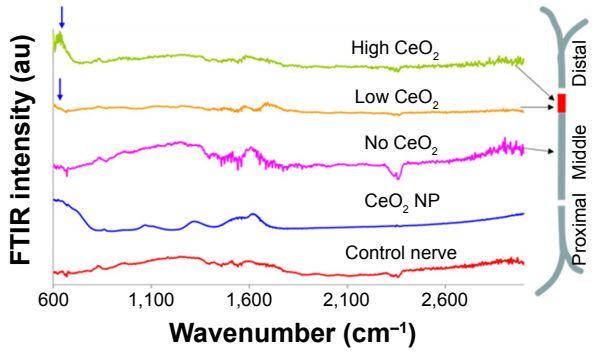

Figure 2 FTIR traces from different regions of CeO_2-treated sciatic nerve of the frog.
Notes: Arrows indicate CeO_2 presence compared to control (CeO_2 NP). Peaks approximately 1,640 cm^{-1} are attributed to the ν_2 band of the hydrogen bond of water.
Abbreviations: FTIR, Fourier transform infrared microscopy; NP, nanoparticle.

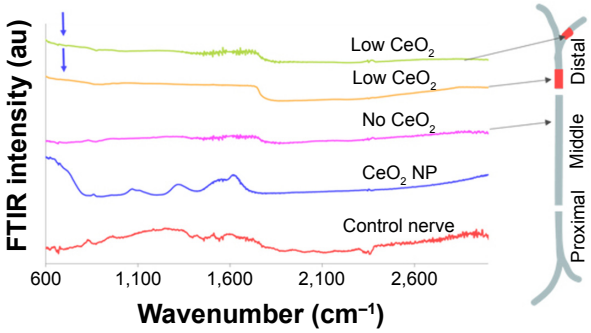

Figure 3 FTIR traces from different regions of CeO_2-treated sciatic nerve of the frog.
Notes: Arrows indicate CeO_2 presence compared to control (CeO_2 NP). Peaks approximately 1,640 cm^{-1} are attributed to the ν_2 band of the hydrogen bond of water.
Abbreviations: FTIR, Fourier transform infrared microscopy; NP, nanoparticle.

chamber was exposed to 0.21 g/L CeO_2, while recordings were made for over 40 hours. NPs were found in none of the three nerves examined.

CeO_2 translocation depends on nerve fiber electrical activity

To demonstrate the relation between nerve fiber electrical activity and NPs translocation, we used another simple method. Four nerves were treated using CeO_2, as already described, but in the absence of electrical stimulation. In this case, the transportation of NPs was minimized. In two out of four cases, few traces of CeO_2 were detected only in the proximal region. In all four nerves, no NPs were detected in either the middle or the distal region. The results of these experiments provide a clear indication that the translocation of NPs depends not only on the integrity of the nerve axons, but also on their electrical activation.

SiO_2 also translocates within the peripheral nerve

In this study, four nerves were exposed to SiO_2 NPs, as already described. In three out of four nerves exposed to SiO_2, traces of NPs were observed in very narrow bundles of 2–3 mm of the distal region of the sciatic nerve, in accordance to the observation for CeO_2.

In Figure 4, the FTIR traces of a nonexposed nerve (control nerve) and of the SiO_2 NPs are shown as negative and positive controls, respectively. No NPs were detected in the middle and distal parts of the nerve. However, in the distal part, 5 mm before the end of the nerve, an area with high SiO_2 presence was detected (trace high SiO_2) following a low one (trace low SiO_2). Prior to this region, and similar to the other areas of the nerve, NPs were not detected (trace no SiO_2).

To provide convincing evidence that our FTIR signal was generated by SiO_2 NPs, parts of the nerve with strong signal

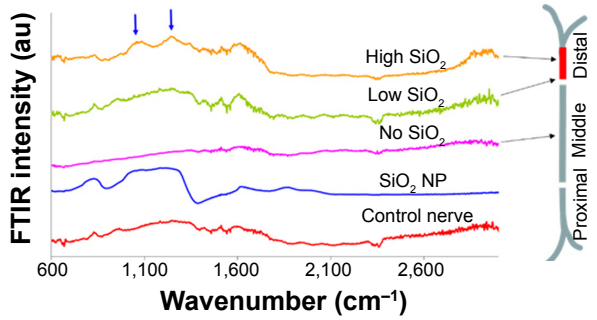

Figure 4 FTIR traces of different SiO_2 treated nerve regions.
Notes: Arrows indicate SiO_2 presence. Peaks approximately 1,640 cm^{-1} are attributed to the ν_2 band of the hydrogen bond of water.
Abbreviations: FTIR, Fourier transform infrared microscopy; NP, nanoparticle.

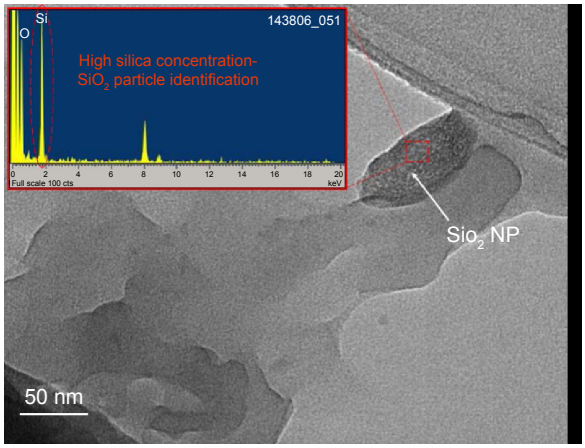

Figure 5 TEM image of the teased and dried nerve fibers, depicting a SiO_2 NP.
Abbreviations: NP, nanoparticle; TEM, transmission electron microscope.

were examined using TEM. A SiO_2 NP from these studies is shown in Figure 5. The TEM images depict spherical dense particle morphology with diameter size distribution between 30 and 120 nm and amorphous crystallinity, all concordant with SiO_2 presence.

Discussion

NPs are widely investigated as drug delivery vehicles in nanomedicine. We investigated the translocation ability of two commonly used NPs, namely CeO_2 and SiO_2, in a model peripheral nerve, the ex vivo preparation of the frog sciatic nerve. Our results indicate that CeO_2 and SiO_2 NPs, with a mean diameter of 120 and 140 nm respectively, translocate along the nerve fibers with an average speed of 0.45–0.58 mm/h. This speed is closer to the slow axonal transport rate (0.072 mm/h) than the fast one (8–10 mm/h). A similar transportation rate, of 1.9 mm/h, has been reported for the Herpes simplex virus-1 in the same preparation.[34] It is possible is that the same transport mechanism is involved in both cases. The relatively large size of CeO_2 and SiO_2 may explain the slower speed compared to the virus.

A key observation of our study has been the detection of a narrow band in the FTIR spectrum, indicating the presence of NP aggregates usually within one of the 1 mm segments in the distal or middle regions of the nerve. The absence of NPs, as characterized by FTIR, can also be defined as low NP quantity in other regions. FTIR spectroscopy characterizes a sample by the absorption peaks of its asymmetric molecular vibrations. The nerve sample exhibits its characteristic control FTIR spectrum, while on the other hand in the NPs case, the collective spectrum of the control and the NPs incorporated in the nerve matrix is presented; thus, the resolution capability for NP presence is limited to

NP quantities that can distinct from the control background. There may be at least two explanations for the narrow band formation. One possibility is that the anterograde transport mechanism requires an aggregate, in other words a "critical NP mass", to operate. If this hypothesis is true, NPs should be present, but below the detection threshold in the proximal segment, absent until the detection site, and the aggregation rate should be slow enough to allow a second, observable band within our 36-hour protocol. Another possibility is that there is a block at the site where the band is detected, and translocated NPs merely aggregate at that point. In this case, NPs should be present, at concentrations below detection, along the length of the nerve up to the detection site. Time and concentration dependence experiments will help to shed light on this interesting phenomenon.

The route of NPs translocation has also been investigated in our study. NPs are transported through the axon and not by other structures of the nerve as the damaged axon experiments have demonstrated. Evidence toward this conclusion has been also provided by the results of the experiments where the whole middle part of the desheathed nerve was exposed to 0.21 g/L CeO_2 with no observed penetration or transportation through either myelin or nodes of Ranvier. The same experiment also demonstrated that the application of NPs at this concentration has no toxic effect on the nerve at the concentration. In other in vitro studies, it has been shown that the number of NPs impacts cytotoxicity.[39]

We have also demonstrated that electrical activation is required for effective transportation. In similar ex vivo frog sciatic nerve experiments, repetitive action potentials have been shown to retard mitochondrial motility through nodes of Ranvier by reducing the number of mobile mitochondria, reducing the velocity, and increasing the pause duration in a Ca^{2+}-dependent manner.[35] Apparently, NP translocation depends on a different mechanism which is facilitated by electrical activation. Further studies are required to investigate this interesting phenomenon.

Our ex vivo nerve preparation constitutes a valuable tool for studying a number of important questions regarding axonal transportation of NPs. The study can be easily extended to other types of NPs, and it can also be used to investigate the relation of NPs size with speed of axonal transport and further to estimate the optimum diameter for maximum speed. The size is an important issue because it may determine the transportation rate of the maximum load. Our methodology is also a useful tool for the pharmacological study of various parameters, eg, drugs diluted in the perfusion chamber, ionizing radiation, and temperature, which may affect the axonal transport of NPs. Furthermore, an investigation is in preparation to assess the movement of NPs in the nerve fibers of mammals, and more specifically in rats. Results from mammalian tissues will provide mechanism insights closer to the human conditions.

Conclusion

Using an ex vivo preparation of the frog sciatic nerve, we have demonstrated that two commonly used NPs, CeO_2 and SiO_2, are transported through the nerve with a speed in the range of the slow transportation rate. The movement depends on axonal integrity and electrical activity. No neurotoxic effects were shown for the CeO_2 concentration tested even after long hours of exposure. Our preparation is advantageous for studying various aspects of axonal transportation of NPs.

Disclosure

The authors report no conflicts of interest in this work.

References

1. Lorentzou S, Kastrinaki G, Pagkoura C, Konstandopoulos AG. Oxide nanoparticles for hydrogen production from water-splitting and catalytic oxidation of diesel exhaust emissions. *Nanosci Nanotechnol Lett*. 2011;3:697–704.
2. Zarvalis D, Lorentzou S, Konstandopoulos AG. Diesel exhaust emission control. *SAE SP*. 2009;2254:143–153.
3. Konstandopoulos G, Lorentzou S. In: Vayssieres L, editor. *Invited Chapter on Solar Hydrogen and Nanotechnology*. New York, NY: John Wiley & Sons; 2010.
4. Lorentzou S, Pagkoura C, Zygogianni A, Kastrinaki G, Konstandopoulos AG. Catalytic nano-structured materials for next generation diesel particulate filters. SAE Technical Paper, 2008-01-0417.
5. Dilnawaz F, Sahoo SK. Therapeutic approaches of magnetic nanoparticles for the central nervous system. *Drug Discov Today*. Epub June 21, 2015.
6. Leite PE, Pereira MR, Granjeiro JM. Hazard effects of nanoparticles in central nervous system: searching for biocompatible nanomaterials for drug delivery. *Toxicol In Vitro*. 2015;29(7):1653–1660.
7. Schulte PA, Geraci CL, Murashov V, et al. Occupational safety and health criteria for responsible development of nanotechnology. *J Nanopart Res*. 2014;16(1):2153.
8. Oszlánczi G, Papp A, Szabó A, et al. Nervous system effects in rats on subacute exposure by lead-containing nanoparticles via the airways. *Inhal Toxicol*. 2011;23(4):173–181.
9. Papaioannou E, Konstandopoulos AG, Morin JP, Preterre D. A selective particle size sampler suitable for biological exposure studies of diesel particulate. SAE Technical Paper Number 2006-01-1075 (SP-2024), 2006:389–399.
10. Elder A, Gelein R, Silva V, et al. Translocation of inhaled ultrafine manganese oxide particles to the central nervous system. *Environ Health Perspect*. 2006;114:1172.
11. Gramowski A, Flossdorf J, Bhattacharya K, et al. Nanoparticles induce changes of the electrical activity of neuronal networks on microelectrode array neurochips. *Environ Health Perspect*. 2010;18:1363–1369.
12. Kang C, Yuan X, Zhong Y, et al. Growth inhibition against intracranial C6 glioma cells by stereotactic delivery of BCNU by controlled release from poly (D,L-lactic acid) nanoparticles. *Technol Cancer Res Treat*. 2009;8:61–70.

13. Sharma HS, Sharma A. Nanoparticles aggravate heat stress induced cognitive deficits, blood–brain barrier disruption, edema formation and brain pathology. *Prog Brain Res*. 2007;162:245–273.
14. Oberdörster G, Elder A, Rinderknecht A. Nanoparticles and the brain: cause for concern? *J Nanosci Nanotechnol*. 2009;9:4996–5007.
15. Takenaka S, Karg E, Roth C, et al. Pulmonary and systemic distribution of inhaled ultrafine silver particles in rats. *Environ Health Perspect*. 2001; 109(4):547–551.
16. Tin-Tin-Win-Shwe, Yamamoto S, Ahmed S, Kakeyama M, Kobayashi T, Fujimaki H. Brain cytokine and chemokine mRNA expression in mice induced by intranasal instillation with ultrafine carbon black. *Toxicol Lett*. 2006;163(2):153–160.
17. Wang J, Liu Y, Jiao F, et al. Time dependent translocation and potential impairment on central nervous system by intranasally instilled TiO_2 nanoparticles. *Toxicology*. 2008;254:82.
18. Wang J, Chen C, Liu Y, et al. Potential neurological lesion after nasal instillation of TiO_2 nanoparticles in the anatase and rutile crystal phases. *Toxicol Lett*. 2008;183:72.
19. Barrios FA, Gonzalez L, Favila R, et al. Olfaction and neurodegeneration in HD. *Neuroreport*. 2007;18(1):73–76.
20. Salonen J, Kaukonen AM, Hirvonen J, et al. Mesoporous silicon in drug delivery applications. *J Pharm Sci*. 2008;97:632–653.
21. DeLouise LA, Miller BL. Enzyme immobilization in porous silicon: quantitative analysis of the kinetic parameters for glutathione-S-transferases. *Anal Chem*. 2005;77(7):1950–1956.
22. Létant SE, Hart BR, Kane SR, et al. Enzyme immobilization on porous silicon surfaces. *Adv Mater*. 2004;16:689–693.
23. Létant SE, Kane SR, Hart BR, et al. Hydrolysis of acetylcholinesterase inhibitors – organophosphorus acid anhydrolase enzyme immobilization on photoluminescent porous silicon platforms. *Chem Commun*. 2005; 7:851–853.
24. Anglin EJ, Schwartz MP, Ng VP, et al. Engineering the chemistry and nanostructure of porous silicon Fabry–Pérot films for loading and release of a steroid. *Langmuir*. 2004;20:11264–11269.
25. Charnay C, Begu S, Tourne-Peteilh C, Nicole L, Lerner DA, Devoisselle JM. Inclusion of ibuprofen in mesoporous templated silica: drug loading and release property. *Eur J Pharm Biopharm*. 2004;57: 533–540.
26. Kaukonen AM, Laitinen L, Salonen J, et al. Enhanced in vitro permeation of furosemide loaded into thermally carbonized mesoporous silicon (TCPSi) microparticles. *Eur J Pharm Biopharm*. 2007;66:348–356.
27. Salonen J, Laitinen L, Kaukonen AM, et al. Mesoporous silicon microparticles for oral drug delivery: loading and release of five model drugs. *J Control Release*. 2005;108:362–374.
28. Celardo I, Pedersen JZ, Traversa E, et al. Pharmacological potential of cerium oxide nanoparticles. *Nanoscale*. 2011;3:1411–1420.
29. Xu C, Qu X. Cerium oxide nanoparticle: a remarkably versatile rare earth nanomaterial for biological applications. *NPG Asia Mater*. 2014; 6:e90.
30. Kim CK, Kim T, Choi IY, et al. Ceria nanoparticles that can protect against ischemic stroke. *Angew Chem Int Ed Engl*. 2012;51: 11039–11043.
31. Chen JP, Patil S, Seal S, et al. Rare earth nanoparticles prevent retinal degeneration induced by intracellular peroxides. *Nat Nanotechnol*. 2006; 1:142–150.
32. Ma JY, Zhao HW, Mercer RR, et al. Cerium oxide nanoparticle-induced pulmonary inflammation and alveolar macrophage functional change in rats. *Nanotoxicology*. 2011;5:312–325.
33. Ma JY, Mercer RR, Barger M, et al. Induction of pulmonary fibrosis by cerium oxide nanoparticles. *Toxicol Appl Pharmacol*. 2012;262: 255–264.
34. Maratou E, Theophilidis G, Arsenakis M. Axonal transport of herpes simplex virus-1 in an in vitro model based on the isolated sciatic nerve of the frog *Rana ridibunda*. *J Neurosci Methods*. 1998;31:75–78.
35. Andreou A, Dabarakis N, Kagiava A, Kosmidis EK, Geronikaki A, Theophilidis G. Assessing the effects of three dental impression materials on the isolated sciatic nerve of rat and frog. *Toxicol In Vitro*. 2007;21: 103–108.
36. Zalachoras I, Kagiava A, Vokou D, Theophilidis G. Assessing the local anesthetic effect of five essential oil constituents. *Planta Med*. 2010;76: 1647–1653.
37. Stys PK, Ransom BR, Waxman SG. Compound action potential of nerve recorded by suction electrode: a theoretical and experimental analysis. *Brain Res*. 1991;546:18–32.
38. Karadimitra K, Papaioannou E, Konstandopoulos AG. Oxidation of diesel particulate in catalytic filters coated by aerosol spray pyrolysis. *J Aerosol Sci*. 2001;32:233–234.
39. Mendes LP, Delgado JM, Costa AD, et al. Biodegradable nanoparticles designed for drug delivery: the number of nanoparticles impacts on cytotoxicity. *Toxicol In Vitro*. 2015;29:1268–1274.